Proceedings Paper:

Sun, Y. orcid.org/0000-0001-6129-4290 and Ball, E.A. orcid.org/0000-0002-6283-5949 (2022) Deep learning applied to automatic modulation classification at 28 GHz. In: Arai, K., (ed.) Intelligent Systems and Applications: Proceedings of the 2022 Intelligent Systems Conference (IntelliSys) Volume 1. 2022 Intelligent Systems Conference (IntelliSys), 01-02 Sep 2022, Amsterdam, The Netherlands. Lecture Notes in Networks and Systems, 1 (LNNS 542). Springer International Publishing , pp. 403-414. ISBN 9783031160714

https://doi.org/10.1007/978-3-031-16072-1_30

Deep Learning Applied to Automatic Modulation Classification at 28 GHz

Yilin Sun[1] and Edward A Ball[2]

[1] The University of Sheffield, Sheffield, S1 4ET, UK
[2] The University of Sheffield, Sheffield, S1 4ET, UK
ysun57@sheffield.ac.uk

Abstract. Automatic Modulation Classification (AMC) as a rapidly evolving technology, is employed in software defined radio structures, especially in 5G and 6G technology. Deep Learning (DL) can provide novel and efficient technology for modulation classification, especially for systems working in low Signal to Noise Ratio (SNR). In this article, we describe a dynamic system for the Millimeter wave (mmW) band, which is not reliant on received signal phase lock and frequency lock. It employs DL to classify the modulation types for different received SNR. In this model, a new method named Graphic Representation of Features (GRF) is proposed, which presents the statistical features as a spider graph for DL. The RF modulation is generating by a lab signal generator, sent through antennas and then captured by an RF signal analyser. In the results from the system with the GRF techniques we observe an overall classification accuracy of 56 % for 0 dB SNR and 67 % at 10 dB SNR, compared to a random guess accuracy of 25 %. The results of the system at 28 GHz are also compared to our previous work at 2 GHz.

Keywords: Automatic Modulation Classification, Deep Learning, Millimeter wave.

1 Introduction

Improvements to radio spectrum usage efficiency are becoming increasingly important, with the evolution of digital communication systems. Dynamic Spectrum Access (DSA) is a critical technique for meeting this need, requiring spectrum sensing and signal classification. In this scenario, the modulation classification performs a significant role and can be widely used in a range of applications, including software defined radio system, and radar and military communications [1], [2]. There is a high demand for radio frequency (RF) bands. In the crowded spectrum situation, the Automatic Modulation Classification (AMC) [3] technology can respond to the requirements, optimising signal detection and subsequent demodulation when multiple complex / unknown signals are to be handled, or for cognitive radio primary-user detection. Radio spectrum is a valuable resource, AMC is method of identifying the users off the spectrum as well as unused spectrum [4].

This work concentrates on modulation classification provided by different methods in the deep learning area. Signals can appear like noises at very low Signal to Noise Ratio (SNR). The purpose of this work is to develop the accuracy of classification in the low SNR area with more efficient methods. With the improvement of Artificial Intelligence (AI) technology, many areas have achieved new progress by this novel area [5]. Classification of modulation types based on statistical properties of signals is common in classic statistical machine learning approaches [6]. From this, Deep Learning (DL) working as a subproject of machine learning, advanced to a new level by incorporating the essence of biological information processing systems [7]. In image classification, DL is employed as an efficient technique [8]. In our work, we develop a model using image classification from DL technology, utilising the Graphic Representation of Features (GRF) to represent the statistical features of the signals. The GRF method benefits from both statistical features and image classification. After presenting the modulated signals in GRF, they are tested by the pre-trained network with the existing advanced image classifiers. Transfer Learning (TL) [9] is introduced as an effective AI technology in this model. Several TL networks are compared in this work. For the GRF, *spider graphs* of the statistical features provide a new way to classify the signals. The model is utilised to detect the modulated signals from -10 dB SNR to 20 dB SNR in the 28 GHzmmW band.

In the previous research, Maximum-likelihood decision theory is used as a critical method [10]. PSK and QAM signals are distinguished with accuracy of 90 % above 9 dB SNR [11]. For the pattern recognition algorithms, the features of signals are involved in the models, where high order cumulants play a critical role in the AMC algorithm. After extracting the efficient features, a Support Vector Machines (SVM) [12] is applied in the recognition process. The accuracy can reach to 96 % at 10 dB SNR for 200 samples [13]. But the probability of correct classification is between 50 % to 70 % at around 0 dB SNR, suggesting a need for more improvement. Compared to the previous classifiers, the binary hierarchical polynomial classifiers are also proposed, with the probability of correct classification of 56 % at 0 dB SNR with 1000 symbols [14]. Hence, there is still the challenge to optimise the AMC system, especially at low SNR.

This work will introduce the new systems with DL technology which is proposed by utilising the GRF, which benefit from the statistical features and image classification with DL. In this system, Convolutional Neural Network, GoogleNet [15], SqueezeNet [16] and Inception-v3 [17] are trialled and compared. We develop the recognition images by extracting the statistical features for the GRF and the constellation graphs are captured from the received signals directly. By using pre-existing neural networks aimed at generic image classification, we leverage this existing technology but repurpose it for modulation classification and thereby also assess its suitability.

There are five key contributions of this work. For our first contribution, we make the assessment of TL, using the pretrained neural network for the system. The good usage of the TL reduces the complexity of calculation and improves the accuracy of modulation classification. For our second contribution, we develop and assess the novel method named Graphic Representation of Features (GRF) to indicate the statistical features of modulation types, represented graphically and used as image classification data. This method takes the advantages of both statistical characterisation and image classification. As our third contribution, we compare the results of testing conducted and radiated data at 28 GHz in our system to find the possibility to improve the robust of wireless communications. Our fourth contribution is the overall assessment of generic DL image classifiers as applied to communications AMC usage. Our final contribution is to compare the results for our technique at 28 GHz with the detection accuracy for lower frequency carriers, in our previous work [18].

In the following parts, we will introduce the system model, classification method, and finally discuss results and performance.

2 System Model and Problem Description

2.1 RF Signal Description

The received signal in baseband is defined with r(t) and it is given by (1).

$$r(t) = s(t) + n(t) \tag{1}$$

Here, $s(t)$ is the original signal which transmits through the additive white Gaussian noise (AWGN) channel, and *n(t)* represents the noise applied to the signals.

With the demand of features calculation and analysis, the raw data should be represented by convention, using in-phase and quadrature components (I/Q), (2).

$$a[i] = a_I[i] + j * a_Q[i] \tag{2}$$

Hence, the signals are composed of in-phase and quadrature components, which can represent the characters of their constellation diagrams. The constellations are captured and observed before the subsequent experiments. The statistical features are calculated from this data. Furthermore, the data captured by signal analyser is also read as I/Q data [19].

The four kinds of modulated signals investigated and applied in this work are: BPSK, QPSK, 8PSK and QAM16. There are 5000 symbols utilised, sampled at the rate of 4 samples per symbol.

In this work, signals are considered from -10 dB to 20 dB SNR. Note that the focus of previous works was on the classification above 10 dB SNR [20]. The SNR value less than 0 dB also should be tested to enhance the performance in discriminating between the four modulation types. We have developed the system from -10 dB to 20 dB SNR to provide a comprehensive dataset.

2.2 Modulation Constellations

We now show the constellations graphs in this section to help display the characteristics. Although in this work, we are utilising the statistical features, some of the features also describe the characteristics of shape of the modulated signals. Fig.1 shows the constellations of conducted data collected from the lab as examples of the four modulation types (BPSK, QPSK, 8PSK, QAM16) at 10 dB SNR at 28 GHz.

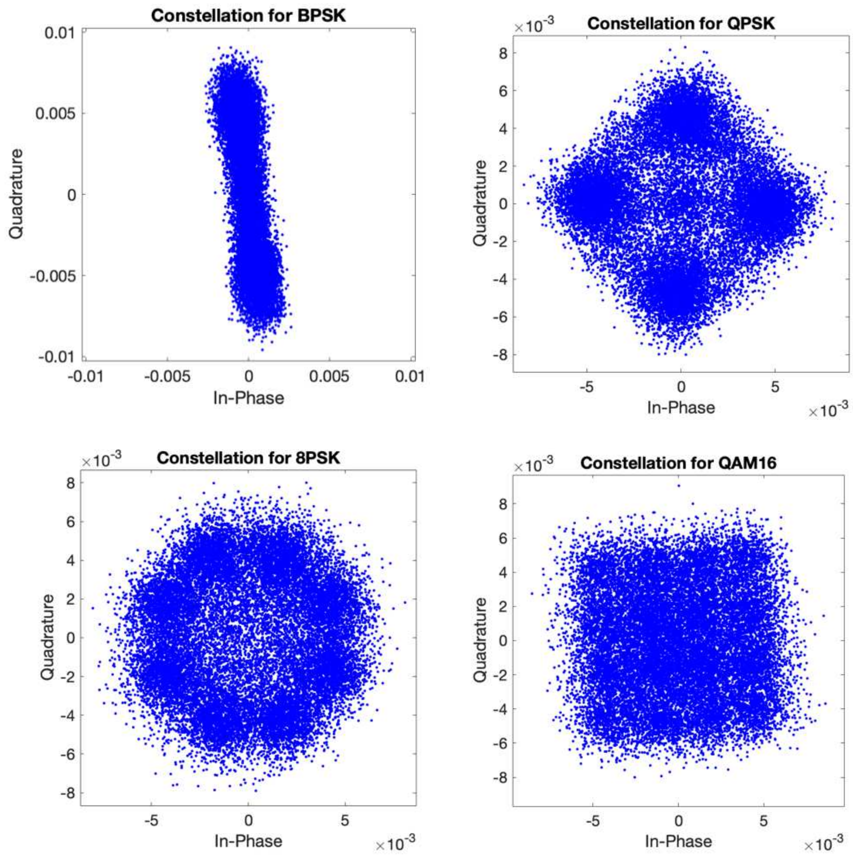

Fig. 1. 28 GHz constellations of captured conducted data.

Fig.1 shows the constellations diagrams of conducted data. At 10 dB SNR, the underlying constellation types are still identifiable and clear. However, at low SNR levels, it becomes hard to distinguish the characteristics. The statistical features are thus introduced to the AMC systems.

2.3 Statistical Features for the Spider Graph representation

The common statistical methods of machine learning are proposed in the previous research to classify digital modulations [21]. The features proposed in the literature for artificial intelligence technologies will also now be considered. The statistical models can obtain the results by capturing the statistical features from the four modulation types from -10dB to 20 dB SNR. The useful features in our earlier paper [18] and include the standard deviation of the signal instantaneous normalised amplitude, σ_{aa}; the maximum value of power spectral density (PSD), γ_{max}; the cumulants of signals, C_{20}, C_{40}, C_{41}, C_{42}, C_{63}, C_{80}; Kurtosis, K; Skewness, S; the ratio of peak-to-rms, *PR*; the ratio of peak-to-average of the signal, *PA*. Some of them also describe the characteristic of the signals.

$$K = \left|\frac{E[(a-E[a])^4]}{E[(a-E[a])^2]^2}\right| \tag{3}$$

For example, Kurtosis is extracted by (3), which describes the steepness or flatness of the distribution of signals [22].

$$S = \left|\frac{E[(a-E[a])^3]}{E[(a-E[a])^2]^{3/2}}\right| \tag{4}$$

Skewness is extracted by (4), which describes the position of the tapering side of the distribution of signals. PA and PR indicate the shape of different signals in detail. We test these statistical features with the collected data in the next section, to find the appropriate and necessary features to build the GRF system.

3 Classification Method

3.1 System structure

In this work, the system employs DL with GRF. The statistical features need to be analysed and selected to work after collecting raw data. GRF is our new developed method to plot the statistical character graphically. In this method, we calculate the data from the dynamic receiving system without phase and frequency lock, to indicate the characteristics in a stable way. After generating the graphs with GRF, we use the pretrained network with existing advanced image classifiers. The classification system is represented Fig. 2. The statistical features of the received signals can be calculated and plotted in the spider graphs, which represents the graphical features.

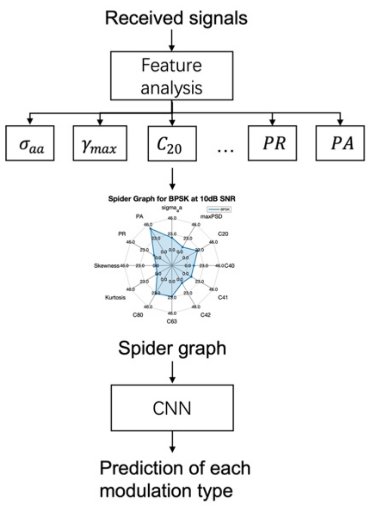

Fig. 2. DL system with GRF

After input to the spider graphs, we can find the prediction of the modulation types. In this work, we use the conducted data as the training dataset. Conducted data and radiated data are then used for testing datasets.

3.2 Graphical Representation of Features (GRF)

Based on the features from our earlier work [18], all the features are calculated for the four modulation types. Fig. 3 shows all statistical features of the four modulated signals at 10 dB SNR at 28 GHz. The features are represented in one graph, some of the features are displayed in logarithmic form, such as σ_{aa}, X_2, γ_{max}, which is a clear way to visualise the magnitude data differences. According to Fig. 3, it is obvious that β, σ_{dp}, σ_v, v_{20}, X, X_2, and C_{21} cannot help to classify the modulations (BPSK, QPSK, 8PSK and QAM16) – the difference of the values of these statistical features are insignificant.

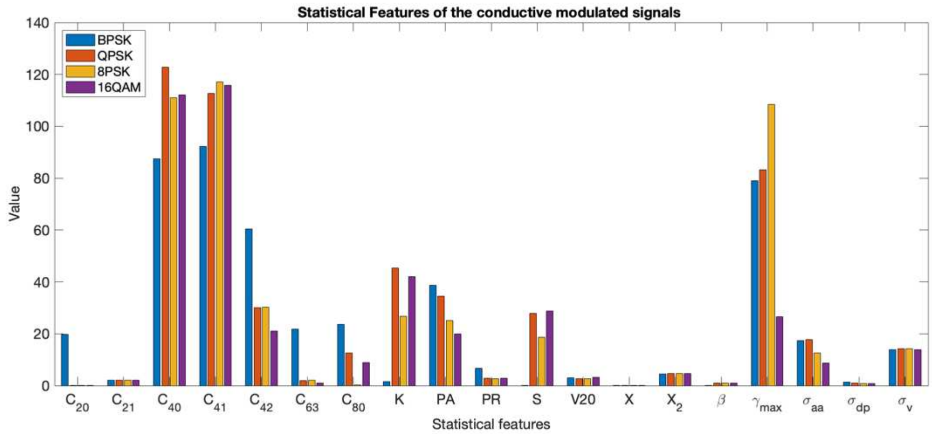

Fig. 3. Features of the 28 GHz conducted modulated signals at 10 dB SNR.

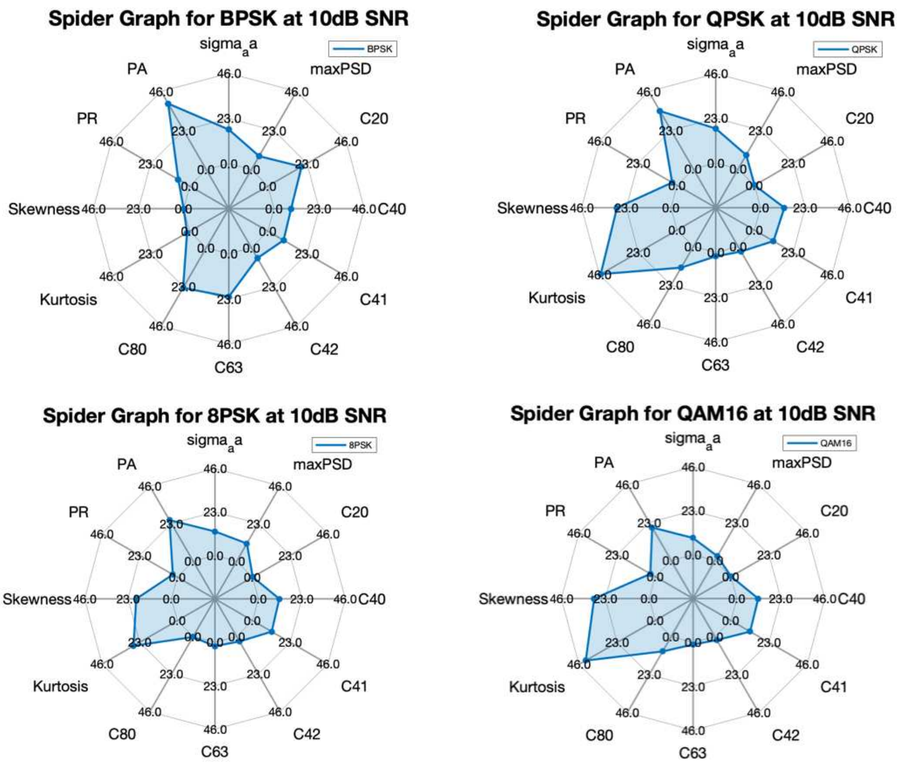

Fig. 4. Spider Graphs of the 28 GHz conducted modulated signals at 10 dB SNR.

Fig. 4 shows statistical features applied in the spider graph. Based on the previous analysis in Fig.3, the twelve features of the modulated signals are selected. The features are employed as the axes of the spider graph- each modulation type can then display the values in the graph. The spider graphs turn the statistical features into one representation and represent the collected statistical features in a graphic way. To label the value of the features in the same common graph required use of the log function for some of the features, where appropriate. As seen in Fig. 4, each modulated signal shows a different shape of representation. After collecting the graphs, all the graphical representations are used for Neural Network with image classification.

3.3 Deep Learning Networks

Deep Learning is an efficient way to improve the performance of AMC. In this section, four Convolutional Neural Network (CNN) models are introduced, a simple CNN developed from the Iris case [23] with multiple layers, the SqueezeNet model [16], the GoogleNet model and the Inception-v3 model [24]. The last three models are pretrained networks, which are also known as TL. We pre-process the signals and obtain the GRF to create the training dataset and testing dataset for CNN.

As shown in Fig. 5, a basic example of CNN structure is built with convolutional layers and dense fully connected layers. The convolutional layers can extract the characters of the signals and generate the feature map. The features can then be learned by the sequential layers. Finally, the categorization results are displayed.

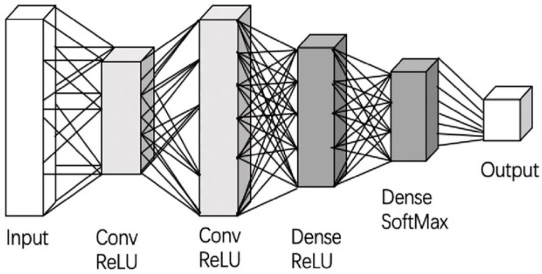

Fig. 5. Example structure of a Neural Network.

CNN. This model is designed as an extension of the Iris recognition case with fifteen layers in total. Following three convolutional layers are the batch normalisation layers and ReLu layers. Between the other three blocks, two max-pooling layers are added to down-sample the input data and limit the risk of overfitting. The filters of convolutional layers can extract the physical features of the images, such as the profile and grayscale. In this case, the convolutional layer is crucial in its ability to classify the images. The batch normalisation layers can normalise the input channel and the threshold can be calculated to the elements by the ReLu layers [25].

Transfer Learning Models. The SqueezeNet contains 68 layers, and the size of input image of the network is 227-by-227 pixels [16]. The GoogleNet includes 144 layers and is pretrained to classify the images into 1000 categories. The size of input image is 224-by-224 pixels [15]. The Inception-v3 is comprised of 315 layers and has been trained distinguish 1000 categories among millions of images [17]. The size of input image is 299-by-299 pixels. Before feeding to the models, images are required to be resized to satisfy the input criteria. To best suit our work, the final learning layers are modified, only producing 4 outputs for each modulation types. 70 % of the GRF images in our experiments are used as training, 20 % of images for the validation process and the remaining 10 % used for testing [26]. We set the system to rotate the images from -90 to 90 degree steps and rescale them randomly from 1 to 1.5, which can assist increase the quantity of training data and avoid overfitting [27].

4 Evaluated Performance

This section presents the results from the different classification networks. All the detecting systems are based on the DL technology. The high order cumulants are employed for this system as the second classification process to be trialled. The Kurtosis, Skewness, PR, and PA can describe the shape of the signals. The system uses conducted data and radiated data collected by horn antenna. In this work, different DL structures are compared. We only use conductive data as training dataset, but both conducted data and radiated data are tested in classification.

In Fig. 6, the results are shown from the four CNN models. The CNN developed using the Iris case performs worse than other traditional DL methods. This is likely due to the structures and coefficients of this CNN variant being potentially very sensitive and thus will significantly influence the classification system.

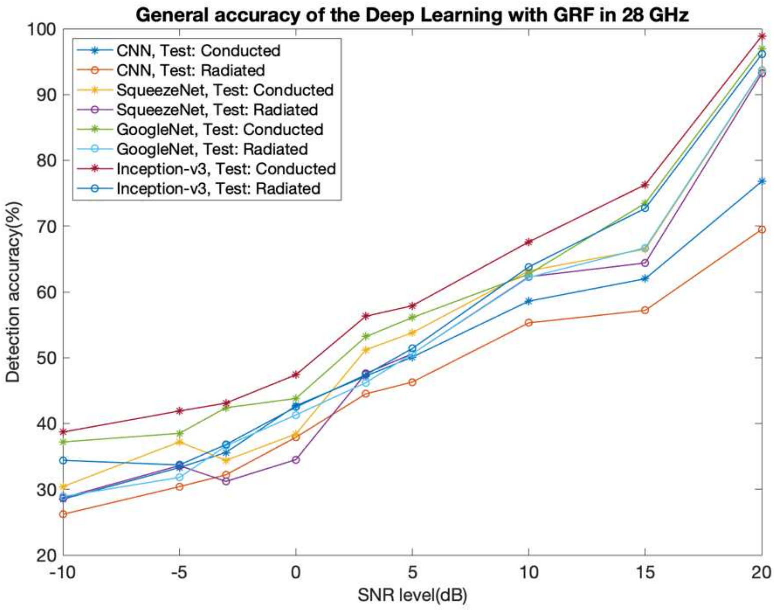

Fig. 6. General accuracy of DL with GRF over different SNR levels at 28 GHz.

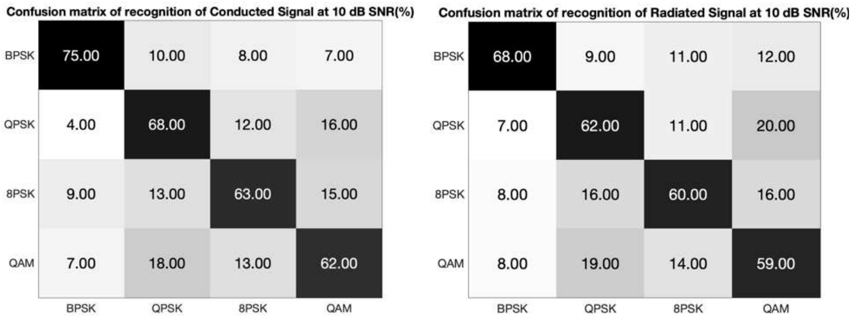

Fig. 7. Accuracy of DL with GRF at 10 dB SNR.

Fig. 7 shows two confusion matrices of the results at 10 dB SNR by using Inception-v3 network. In general, the random guess detection rate would be 25 % (since there are four possible modulation types). This model also provides accuracy slightly higher than random guess at -10 dB SNR, an SNR level well below what most communication system would use.

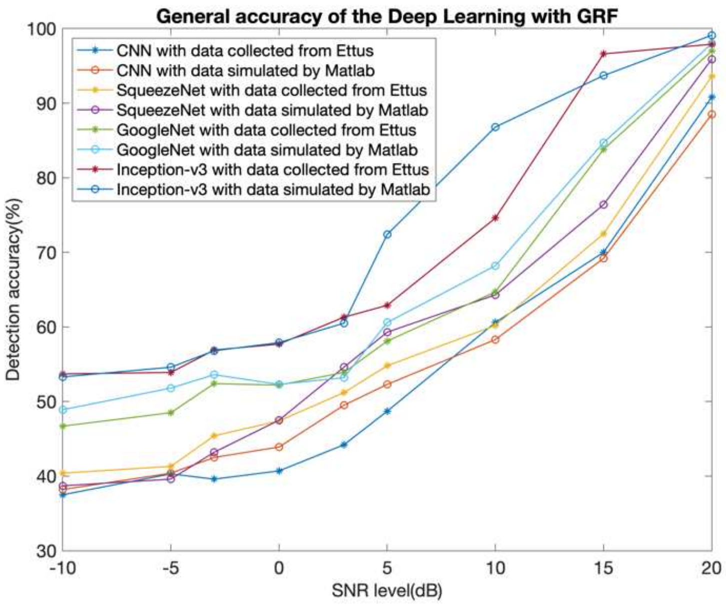

Fig. 8. General accuracy of DL with GRF over different SNR levels at 2 GHz [18].

We also compare the detection accuracy for our technique as applied in [18] at 2 GHz. In that scenario we obtained detection accuracy as in Fig. 8 for various SNR levels. From this, we can see that the detection accuracy using our system at 28 GHz is slightly worse (circa 10 % worse at -10 dB SNR, though this improves as SNR increases). We are investigating possible causes for this difference, which could be due to propagation effects in the lab and the different RF equipment used.

5 Conclusion

In this work, the AMC models based on DL, applied to modulation recognition in a dynamic receiving system without phase and frequency lock in mmW band at 28 GHz are reported. Firstly, we collect conducted and radiated data at 28 GHz and analyse the statistical features. After that, we provide an overview of the GRF method for feature representation. The system utilizes Inception-v3 to obtain the highest accuracy. We then provide a brief comparison between the results at 28 GHz and our earlier results [18] at a lower frequency of 2 GHz and discuss possible causes for differences in classification accuracy. Though the 28 GHz modulation classification performance is circa 10 % lower than with our 2 GHz system, it still is capable of good classification and is significantly better than a random guess probability.

The results also give us stimulus to explore our classifier in higher mmW bands. Therefore, for our future work, we will continue to analyze mmW RF signals and improve applicability of the classifier system in the mmW area.

Acknowledgment

This work was in part supported by a UKRI Future Leaders Fellowship [grant number MR/T043164/1].

References

[1] Kulin, M., Kazaz, T., Moerman, I., De Poorter, E.: ‘End-to-End Learning from Spectrum Data: A Deep Learning Approach for Wireless Signal Identification in Spectrum Monitoring Applications’, *IEEE Access*, 2018, **6**, pp. 18484–18501.

[2] Hamid, M., Slimane, S. Ben, Moer, W. Van, Björsell, N.: ‘Spectrum Sensing Challenges: Blind Sensing and Sensing Optimization’, *IEEE Instrum. Meas. Mag.*, 2016, **19**, (2), pp. 44–52.

[3] Zhechen, Z., and Asoke,K,N.: 'Automatic Modulation Classification : Principles, Algorithms and Applications', (New York: John Wiley & Sons, Incorporated, 2015)

[4] Hindia, M.N., Qamar, F., Ojukwu, H., Dimyati, K., Al-Samman, A.M., Amiri, I.S.: ‘On Platform to Enable the Cognitive Radio Over 5G Networks’, *Wirel. Pers. Commun.*, 2020, **113**, (2), pp. 1241–1262

[5] West, N.E., O'Shea, T.: 'Deep architectures for modulation recognition'. Proc. 2017 IEEE Int. Symposium on Dynamic Spectrum Access Networks (DySPAN), Baltimore, USA, 2017, pp. 1–6

[6] Kim, J., Lee, B., Lee, H., Kim, Y., Lee, J.: 'Deep Learning-Assisted Multi-Dimensional Modulation and Resource Mapping for Advanced OFDM Systems'. Proc. 2018 IEEE Globecom Workshops (GC Wkshps), Abu Dhabi, United Arab Emirates, 2019, pp. 1–6

[7] Schmidhuber, J.: 'Deep Learning in neural networks: An overview', Neural Networks, 2015, 61, pp. 85–117.

[8] Chen, H., Wang, Z., Zhang, L.: 'Collaborative spectrum sensing for illegal drone detection: A deep learning-based image classification perspective', *China Commun*., 2020, **17**, (2), pp. 81–92

[9] Gao, Y., Mosalam, K.M.: 'Deep Transfer Learning for Image-Based Structural Damage Recognition', Comput. Civ. Infrastruct. Eng., 2018, 33, (9), pp. 748–768.

[10] Sills, J.A.: 'Maximum-likelihood modulation classification'. Proc. MILCOM 1999. IEEE Military Communications, Atlantic City, USA, 1999, pp. 217–220

[11] Whelchel, J.E., McNeill, D.L., Hughes, R.D., Loos, M.M.: 'Signal understanding: An artificial intelligence approach to modulation classification'. Proc. IEEE Int. Workshop on Tools for Artificial Intelligence, Fairfax, USA, 1989, pp. 231–236

[12] Corinna, C.; Vladimir, V.: 'Support-Vector Networks', Mach. Learn., 1995, 20, pp. 273–297.

[13] Gang, H., Jiandong, L., Donghua, L.: 'Study of modulation recognition based on HOCs and SVM'. Proc. IEEE 59th Vehicular Technology Conf., Milan, Italy, 2004, pp. 898–902

[14] Abdelmutalab, A., Assaleh, K., El-Tarhuni, M.: 'Automatic modulation classification based on high order cumulants and hierarchical polynomial classifiers', Phys. Commun., 2016, 21, pp. 10–18.

[15] Szegedy, C., Liu, W., Jia, Y., et al.: 'Going deeper with convolutions'. Proc. IEEE Conf. on Computer Vision and Pattern Recognition (CVPR), 2015, pp. 1–9

[16] Iandola, F.N., Han, S., Moskewicz, M.W., Ashraf, K., Dally, W.J., Keutzer, K.: 'SqueezeNet: AlexNet-level accuracy with 50x fewer parameters and <0.5MB model size', 2016

[17] Szegedy, C., Vanhoucke, V., Ioffe, S., Shlens, J., Wojna, Z.: 'Rethinking the Inception Architecture for Computer Vision'. Proc. IEEE Conf. on Computer Vision and Pattern Recognition (CVPR), 2016, pp. 2818–2826

[18] Sun, Y., Ball, E.A.: Automatic modulation classification using techniques from image classification. IET Commun. 1– 12 (2022).

[19] O'Shea, T.J., Roy, T., Clancy, T.C.: 'Over-the-Air Deep Learning Based Radio Signal Classification', IEEE J. Sel. Top. Signal Process., 2018, 12, (1), pp. 168–179.

[20] Chen, K.Z., Hu, A.Q.: 'MPSK demodulation algorithm based on pattern recognition'. Proc. Int. Conf. on Neural Networks and Signal Processing, Nanjing, China, 2008, pp. 182–186

[21] Zhang, M., Diao, M., Guo, L.: 'Convolutional Neural Networks for Automatic Cognitive Radio Waveform Recognition', IEEE Access, 2017, 5, pp. 11074–11082.

[22] Lee, J., Kim, B., Kim, J., Yoon, D., Choi, J.W.: 'Deep neural network-based blind modulation classification for fading channels'. Proc. Int. Conf. on Information and Communication Technology Convergence (ICTC), 2017, pp. 551–554

[23] FISHER, R..: 'The use of multiple measurements in taxonomic problems', 1936

[24] Grm, K., Struc, V., Artiges, A., Caron, M., Ekenel, H.K.: 'Strengths and weaknesses of deep learning models for face recognition against image degradations', IET Biometrics, 2018, 7, (1), pp. 81–89.

[25] Alsina-Pages, R.M., Hervas, M., Vilasis-Cardona, X., Vinyoles-Serra, M.: 'QPSK demodulation using cellular neural networks'. Proc. 14th Int. Workshop on Cellular Nanoscale Networks and their Applications (CNNA), 2014, pp. 1–2

[26] O'Shea, T., Hoydis, J.: 'An Introduction to Deep Learning for the Physical Layer', IEEE Trans. Cogn. Commun. Netw., 2017, 3, (4), pp. 563–575.

[27] Peng, S., Jiang, H., Wang, H., Alwageed, H., Yao, Y.D.: 'Modulation classification using convolutional Neural Network based deep learning model'. Proc. 26th Wireless and Optical Communication Conf. (WOCC), 2017, pp. 1–5